Talanta 210 (2020) 120638

Contents lists available at ScienceDirect

Talanta

journal homepage: www.elsevier.com/locate/talanta

A rapid, adaptative DNA biosensor based on molecular beacon-concatenated dual signal amplification strategies for ultrasensitive detection of p53 gene and cancer cells

Zewei Luo[a,b], Ya Xu[b], Zhijun Huang[a,b], Junman Chen[b], Xiaqing Wang[b], Dan Li[b], Yongxin Li[c], Yixiang Duan[a,b,*]

[a] Research Center of Analytical Instrumentation, Key Laboratory of Synthetic and Natural Functional Molecule Chemistry of Ministry of Education, College of Chemistry & Materials Science, Northwest University, Xi'an, 710069, Shaanxi, PR China
[b] Research Center of Analytical Instrumentation, Key Laboratory of Bio-Resource and Eco-Environment of Ministry of Education, College of Life Sciences, Sichuan University, Chengdu, 610065, Sichuan, PR China
[c] West China School of Public Health, Sichuan University, Chengdu, 610065, China

ARTICLE INFO

Keywords:
Catalytic hairpin assembly
Nicking enzyme
DNA biosensor
Molecular beacon
Cancer

ABSTRACT

The cancer diagnosis with single level of biomarkers suffers from limitation of insufficient accuracy. Hence, developing sensitive, rapid and adaptative analytical strategies for double-level biomarkers are essential for improving the accuracy of clinical cancer diagnosis at early stage. Herein, a DNA biosensor was established based on the catalytic hairpin assembly-mediated Y-junction nicking enzyme assisted signal amplification (CHA-YNEASA) circuits, where the two circuits were concatenated by molecular beacon (MB). In absence of target, both the CHA and YNEASA circuits were effectively hindered because of MB's outstanding ability to control signal background. In presence of target, the initiated CHA circuits made enzyme recognition sequences in close proximity to the assisted sequences to open MB, leading to further trigger the YNEASA circuits. Due to the unique design of dual signal amplification strategies, CHA-YNEASA circuits significantly shorten the reaction time, and improve signal-to-background ratio as well as facilitate the analysis process. It was demonstrated that a high sensitivity with limit of detection (LOD) of 0.9 pM for p53 gene detection was obtained just within 23 min by the proposed DNA biosensor. Moreover, mismatched p53 gene at nucleic acid level was effectively discriminated and strong anti-interference capability was achieved. Noticeably, the DNA biosensor was adaptative for designing a cytosensor at cell level using hairpin DNA, containing MUC1 aptamer and initiation strand of CHA-YNEASA circuits, as switch based on modularity principle. The cytosensor is able to measure MUC1 positive breast cancer cells (MCF-7) with the LOD as low as 100 cells/mL. Excellent specificity for MUC1 negative cells, and good anti-interference capability in 10% fetal bovine serum (FBS) were observed by the cytosensor. Therefore, the proposed DNA biosensor is a sensitive, rapid, adaptative platform for detection of double-level biomarkers, offering novel strategy applied for clinical cancer diagnosis.

1. Introduction

The early-stage diagnosis of cancer greatly depends on biomarkers in body fluids. Up to now, a large amounts of bioanalytical platforms have been developed for individual level of cancer biomarkers' detection, for example, the polymerase chain reaction for gene detection [1,2], and the flow cytometry technique for cancer cell analysis [3]. Although those platforms are suitable for single level of cancer biomarkers with high sensitivity, they suffer from some limitations in practical application, such as complex operation, high time-cost and trained personality. Moreover, these analytical techniques are not able to be extended for other levels of cancer biomarker detection. According to recent research, cancer is a complex disease that is related with multilevel, complex physiological and pathological events [4,5]. Currently, single level of biomarker usually can't accurately predict the occurrence and prognosis of cancers. Diagnosis using multilevel biomarkers ranging from genes to cells will strongly improve the predictive capabilities of cancer. Hence, it is desirable to develop a rapid,

* Corresponding author. Research Center of Analytical Instrumentation, Key Laboratory of Synthetic and Natural Functional Molecule Chemistry of Ministry of Education, College of Chemistry & Materials Science, Northwest University, Xi'an, 710069, Shaanxi, PR China.
E-mail address: yduan@nwu.edu.cn (Y. Duan).

https://doi.org/10.1016/j.talanta.2019.120638
Received 21 October 2019; Received in revised form 6 December 2019; Accepted 8 December 2019
Available online 12 December 2019
0039-9140/

adaptative analytical platform for sensitive detection of multilevel biomarkers.

Catalytic hairpin assembly (CHA) circuits are the most promising nucleic acid circuits to amplify signal [7,41]. There are lots of unique advantages for CHA circuits. It can break the fundamental bottleneck of target-to-signal ratio of 1:1 in the traditional DNA hybridization assay and improve sensitivity through signal amplification process with almost zero background [8,9]. Besides, CHA circuits are flexibly integrated with aptamer, making it a highly specific for analysis of multilevel targets, ranging from small molecules [10], nucleic acids [11], proteins [12], and cancer cells [40]. Consequently, CHA circuits have attracted increasing attentions in application of biosensor platform [14,15]. Despite its high signal-to-noise ratio and adaptive character for multilevel biomarkers' analysis, an ideal CHA circuits are able to only amplify the signal by 50 to 100-fold within a few hours [16]. Therefore, the sensitivity and efficiency is insufficient to meet the requirement in cancer diagnosis at early stage.

As a special group of restriction endonuclease, nicking enzyme is capable of recognizing the specific nucleotide sequences and thereby just cut one of the DNA strands in duplex-stranded DNA [17,18]. In a typical signal simplification strategy, which is named as strand displacement amplification (SDA) [19,20], nicking enzyme is coupled with DNA polymerase. To enhance sensitivity, SDA has been integrated into CHA circuits to form dual signal amplification strategies in recent studies [21–23]. Due to higher order signal amplification, the dual signal amplification strategies always provide high sensitivity for target analysis. However, in presence of two kinds of protein enzymes, the circuits design is more difficult and stricter reaction conditions are required. To simplify design, dual signal amplification strategies through combining nicking enzyme assisted signal amplification (NEASA) and CHA circuits were reported without help of DNA polymerase [18,24]. In these dual signal amplification strategies, single-stranded DNA replaced by target initiates NEASA circuits through forming a duplex-stranded DNA containing enzyme recognition sequences, and then the corresponding product triggered the NEASA circuits. The dual signal amplification strategies exhibit high amplification ability, while only a simple reaction system is involved. However, some weaknesses have to address in these circuits. Incorrect assembly of single-stranded DNAs could form duplex-stranded DNA of enzyme recognition sequences and then non-specifically initiate NEASA in the absence of target, causing a relatively high background and false-positive signals. Moreover, in these dual signal amplification strategies, every circuit was performed separately, which is time-consuming analysis and cumbersome from the operational point of view.

As a hairpin-shaped DNA, molecular beacon (MB) has emerged as promising tool for biosensor with a low fluorescent background, because it allows the fluorophore in close proximity to the quencher [25,26]. MB has been employed as a Y-junction nicking enzyme assisted signal amplification (YNEASA) circuits consisting of enzyme recognition and assisted sequences in recent years [27–29]. The YNEASA circuits are triggered only when the enzyme recognition sequences are close to the assisted sequences, leading to a strong ability to control background and enhance signal-to-background ratio [29,31]. In this work, a sensitive, one-step, adaptative DNA biosensor containing MB-concatenated CHA and YNEASA circuits was developed. Our prepared DNA biosensor is simply composed of two hairpins, a MB, and a nicking enzyme. Enzyme recognition sequences were blocked on the hairpin DNAs and separated from the assisted sequences. Low background signal was obtained in absence of target. The presence of target triggers the cascade reaction of CHA. Then, the enzyme recognition sequences were exposed and close to the enzyme assisted sequences to form a Y-junction DNA structure. As a consequence, the YNEASA circuits were efficiently triggered. Benefiting from higher order signal amplification and effective control of background signal, the prepared DNA biosensor performed rapid and sensitive analysis just in one-step process. More importantly, the inherent modularity of the prepared DNA biosensor allows us to readily adapt it to detect double-level biomarkers of p53 gene and MCF-7 cancer cells with high sensitivity, specificity and anti-interference ability. The prepared DNA biosensor has great potential for cancer diagnosis *in vitro* at early stage.

2. Experimental section

2.1. Materials and methods

Nicking enzyme Nt.BbvCl and Cutsmart™ buffer were purchased from New England Biolabs (U.K.). Tris-(hydroxymethyl) aminomethane (Tris) were obtained from Sigma-Aldrich Inc. All oligonucleotides used were synthesized and purified by Shanghai Sangon Biotechnological Co., Ltd. (China), as listed in Table S1. The aptamer@initiation strand (apt@Is) at the concentration of 1 μM was prepared in binding buffer (100 mM PBS, 1 mM Mg^{2+}, pH 7.4). The others at the concentration of 1 μM were prepared in 1 × CutSmart™ buffer (50 mM potassium acetate, 20 mM Tri-acetate, 10 mM magnesium acetate, 100 μg/mL BSA, pH 7.9). Each oligonucleotide was heated to 94 °C for 3 min in metal bath, and then allowed to cool down to room temperature before use.

2.2. Cell lines and cell culture

The MCF-7, SW620, U–2OS, HL-7702, Hep G2 were obtained from the Institute of Biochemistry and Cell Biology, Chinese Academy of Science. MCF-7 cells were cultured in MEM medium supplemented with 2 μg/mL insulin, 10% fetal bovine serum (FBS), 100 U/mL penicilin and 100 μg/mL streptomycin. The other cell lines were maintained in DMEM medium supplemented with 10% FBS, 100 U/mL penicilin and 100 μg/mL streptomycin. All of the cell lines were incubated at 37 °C in a 5% CO_2 humidified atmosphere. Prior to measurements, the cells at log phase were collected in the corresponding medium trypsin digestion. Then, the collected cells were separated from the medium by centrifugation at 1200 r/min for 3 min. The cell sediment was re-suspended in binding buffer. The cell concentration was obtained by cell counter (Millipore Scepter TM, Merck Millipore, USA). The cells were diluted with binding buffer to a contained concentration before use.

2.3. Polyacrylamide gel electrophoresis (PAGE)

In the gel electrophoresis assay, 7.5 μL different reaction products were mixed with 1.5 μL 6 × loading buffer. Then the mixed solutions of 9.0 μL were subjected to 10% polyacrylamide gel (10%, Acr: Bis = 29:1). After run at 120 V for 35 min in 1 × TAE buffer (40 mM Tris-Acetate, 1 mM EDTA, pH 8.3), the gel was stained with 4 S Red Plus Nucleic Acid Stain (Shanghai Sangon Biotechnological Co., China) for 15 min. Then, images were obtained by a C300 system (azure, USA).

2.4. Kinetic analysis

Kinetic analysis of the three DNA biosensors based on CHA-mediated duplex-strand nicking enzyme assisted signal amplification (CHA-DNEASA), the pure CHA, and CHA-YNEASA circuits was performed. In CHA-YNEASA circuits, a reaction solution with total volume of 130 μL contained 75 nM H1, 100 nM H2-12, 200 nM MB1, 7.5 U Nt.*Bbv*CI enzymes, and 1 × CutSmart™ buffer. In pure CHA circuits, 7.5 U Nt.*Bbv*CI enzymes were removed and other reaction conditions were same as CHA-YNEASA circuits. In CHA-DNEASA circuits, 200 nM MB1 were replaced by 200 nM taqman probe (TB) and other reaction conditions were same as CHA-YNEASA circuits. The reaction solution of the three biosensors was placed into quartz cuvette at a constant temperature of 37 °C maintained by low temperature constant temperature circulator (Hanuo Instruments, China) and the corresponding time-depend fluorescence intensity at 522 nm was recorded in presence or absence of 2 nM p53 gene by LS-55 luminescence spectrometer (PerkinElmer, USA).

2.5. Detection of p53 gene

For p53 gene assay, a solution with total system volumes of 130 μL that contained 75 nM H1, 100 nM H2-12, 200 nM MB1, 7.5 U Nt.*Bbv*CI enzyme, and 1 × CutSmart™ buffer were mixed with p53 gene with various concentrations. Then, the mixture was reacted at 37 °C for 23 min in metal bath and then was rapidly placed in ice bath to end the reaction. Subsequently, the solution was added into a 100 μL quartz cuvette and was analysized by a LS-55 luminescence spectrometer (PerkinElmer, USA). The emission spectra ranging from 515 to 650 nm were collected with excitation wavelength at 497 nm.

2.6. Detection of cancer cells

For cancer cell assay, 10 μL cancer cells with various concentrations and 10 μL apt@Is (0.2 μM) were mixed with 30 μL binding buffer. The mixture was then incubated for 2 h under stirring in a thermostatic oscillator. 6.5 μL solution was taken from mixture and then mixed with 8 μL H3, 16 μL H4 and 56 μL MB2 at concentration of 1 μM. Then, 0.75 μL Nt.*Bbv*CI enzyme (100 U/μL) was added quickly. To keep a total system volume of 130 μL, a contained 1 × CutSmart™ buffer was added. After reacted at 37 °C for 23 min, the mixture was rapidly placed in ice bath to stop the reaction. The subsequent procedures were carried out as same as described above.

3. Results and discussion

3.1. Principle DNA biosensor for p53 gene detection

Multi-genes express abnormal in early stage of cancer. As a tumor suppressor, p53 gene is the most commonly mutated genes in human tumors, leading to speed up tumor growth. Here, p53 gene was employed as mode target of cancer biomarker at nucleic acid level. The working principle of the DNA biosensor for p53 gene detection based on CHA-YNEASA is schematically shown in Fig. 1. The DNA biosensor consists of two types of hairpins (H1 and H2), a MB1, and a nicking enzyme (Nt.*Bbv*CI). H1 and H2 in CHA circuits were designed according to previous report with some modifications [8]. The YNEASA circuits include enzyme recognition sequences, assisted sequences, and a nicking enzyme, where enzyme recognition sequences blocked on H1 are separated from the assisted sequences. In absence of p53 gene, the spontaneous hybridization of hairpin H1, H2 and MB1 is kinetically hindered [8] and the two circuits are blocked. In the presence of p53 gene, hairpin H1 is initially opened, and then hybridized with hairpin H2, which finally displaces p53 gene and make it away from H1. The liberated p53 gene is able to trigger other cycles of CHA circuits. Meanwhile, H1–H2 complexes are capable of hybridizing with MB1 to assemble a Y-shaped junction structure, because the whole recognition sequences of nicking enzyme in H1–H2 complexes are in close proximity to the assisted sequences. Then, the YNEASA circuits occurred and MB1 was cut into two fragments (cMB1) by nicking enzyme. The cMB1 would dissociate from H1–H2 complexes due to less stable duplex structure [32,33]. Thus, H1–H2 complexes further hybridized with MB1 to initiate the next cycle of YNEASA circuits.

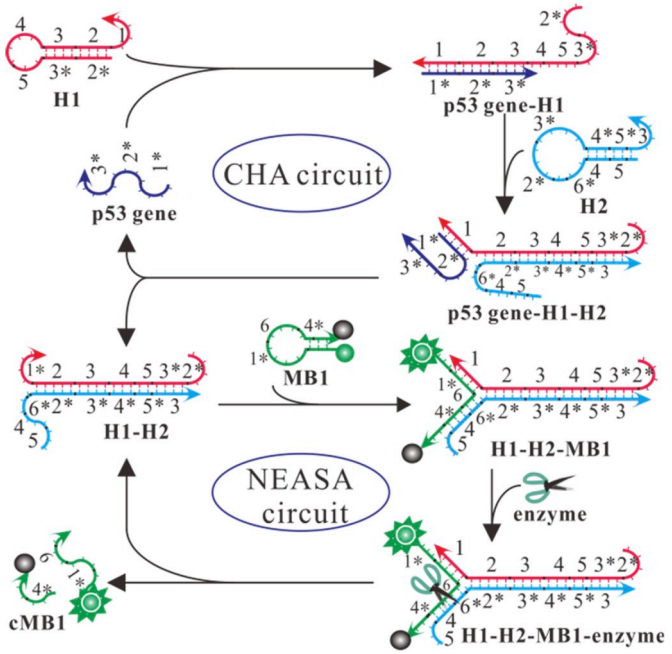

Fig. 1. Working principle of DNA biosensor for p53 gene detection.

The sequences' design process of biosensor is summarized in Fig. S-1 in detail using a modularity principle, which ensures the adaptation of the designed DNA biosensor. The sequences of p53 gene selected from NCBI were divided into three parts (domain 1*, 2* and 3*). The complementary sequences (domain 1, 2 and 3) were fixed according to the rule of base complementary pairing. Part of enzyme recognition sequences (domain 4 and 6*) were fixed according to nicking enzyme Nt.*Bbv*CI used. To keep correct folding structure of DNA used, the left sequences in H1, H2 and MB1 were designed with aid of NUPACK. The corresponding sequences are shown in Table S1.

3.2. Feasibility of DNA biosensor based on CHA-YNEASA circuits

To ensure the feasibility of CHA-YNEASA circuits, each circuit was testified separately. For the CHA circuits in Fig. S-2, in presence of p53 gene, the new formed bands (lanes 5–7) were equivalent to those generated from the annealing of hairpin H1 and H2 (lane 4), indicating that H1–H2 complexes was assembled through CHA circuits. For the YNEASA circuits in Fig. S-3, the brightness of MB1 bands decreased when the annealing of H1 and H2 increased in lanes 6–8, indicating that MB1 was cut into fragments (cMB1) through YNEASA circuits. Fragments (cMB1) were no observed in lines 6–8 of Fig. S-3. Because both fragments (cMB1) is single-stranded DNA structure that aren't stained by 4 S Red Plus Nucleic Acid Stain. Thus, both CHA and YNEASA circuits perform as expected.

The proof-of-concept demonstration of the DNA biosensor was estimated by measuring fluorescence intensity of reaction system, as depicted in Fig. 2A. In p53 gene-free groups, the mixtures of H1/H2/MB1 (curve a) and H1/H2/MB1/enzyme (curve c) exhibit low fluorescence intensity, which is due to the well control of background in CHA and YNEASA circuits. In pure CHA circuits, hairpins were rapidly assembled by catalyst p53 gene. Fluorescence signal generated because the fluorescence group (FAM) departed from quencher group (Dabcyl) to break the fluorescence resonance energy transfer (FRET). Comparing with p53 gene-free groups (curve a), a 311% signal enhancement in fluorescence intensity upon addition of p53 gene was achieved in curve b, assuring high amplification ability of CHA circuits. More importantly, large numbers of MB1 were cleaved into two fragments (cMB1) by introducing nicking enzyme in CHA-YNEASA circuits. Thus, fluorescence and quencher group were separated, causing a remarkable increase of fluorescence intensity. It is demonstrated that a 712% fluorescence signal enhancement is observed in curve d than that in curve c. Compared to pure CHA circuits, the CHA-YNEASA circuits show more than doubled signal-to-background ratio. Gel electrophoresis experiments give similar results for further validation of CHA-YNEASA circuits, as shown in Fig. 2B. In p53 gene-free group (lane 4), no obvious Y-shaped H1–H2-MB1 complexes were observed; while p53 gene-added group (lane 5) produced significant Y-shaped H1–H2-MB1 complexes. By introducing nicking enzyme (lanes 7–9), the brightness of MB1 band showed a decreasing intensity with the increase of p53 gene. The more p53 gene presented, the more H1–H2 complexes and

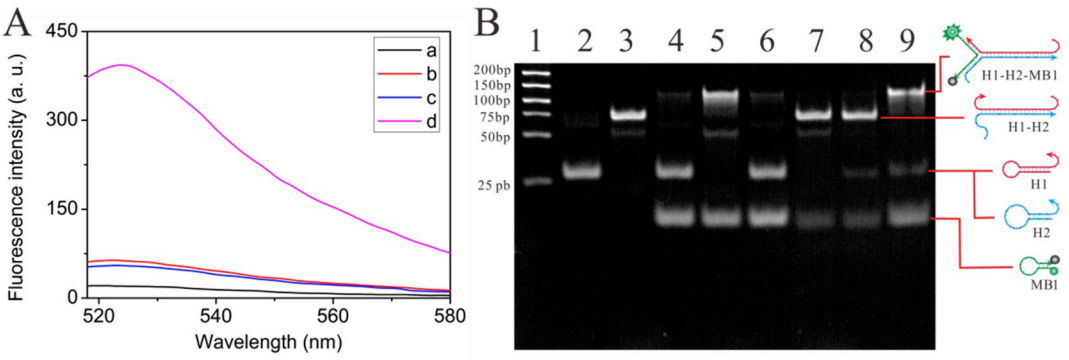

Fig. 2. Feasibility of the DNA biosensor based on CHA-YNEASA circuits. (A) Fluorescence analysis: curve a, 75 nM H1 + 100 nM H2-12 + 200 nM MB1; curve b, 2 nM p53 gene + a; curve c, 7.5 U Nt.*Bbv*CI + a; curve d, 2 nM p 53 gene + c. (B) PAGE analysis: lane 1, DNA ladders; lane 2, 75 nM H1 + 100 nM H2-12; lane 3, 25 nM p53 gene + lane 2; lane 4, 600 nM MB1 + lane 2; lane 5, 25 nM p53 gene + lane 4; lane 6, 5 U Nt.*Bbv*CI + lane 4; lane 7, 25 nM p53 gene + lane 6; lane 8, 12.5 nM p53 gene + lane 6; lane 9, 6.25 nM p53 gene + lane 6.

H1–H2-MB1 complexes were assembled. Then, H1–H2-MB1 complexes were disassembled to form H1–H2 complexes because MB1 was cut into two fragments by nicking enzyme and the responding cleaved fragments (cMB1) were away from H1–H2 complexes. When p53 gene with high concentration (lines 7–8) presented, most of MB1 were cleaved and H1–H2 complexes were formed. While p53 with low concentration (line 9) presented, a fraction of MB1 were cleaved and another fraction of MB1 hybridized with H1–H2 complexes to form H1–H2-MB1 complexes. Thus, the rest of MB1 were observed in line 9 of Fig. 2B. These results demonstrate that CHA-YNEASA circuits are effectively triggered by p53 gene.

3.3. Conditions' optimization

To acquire optimal performance for p53 gene detection by our prepared DNA biosensor, four key factors, including H1 concentration, enzyme amount, MB1 concentration and stem length of H2, were optimized. The results are displayed in Fig. S-4. Firstly, the effect of H1 concentration on the signal of biosensor was examined. As shown in Fig. S-4A, the fluorescence signal gradually increases with H1 concentration increasing from 25 nM to 75 nM and reaches a plateau thereafter; while, the background also increases when the H2 concentration goes from 75 nM to 125 nM. In low concentration range of H1, the reaction efficiency of CHA-YNEASA circuits was limited to some extent; while in high concentration of H1, the unreacted H1 may incorrectly hybridize with other DNA molecules to generate background signal. Therefore, the H1 concentration of 75 nM was selected for the subsequent experiments. As shown in Fig. S–4B and Fig. S–4C, the enzyme amount and MB1 concentration show same tendency in terms of their effect on the biosensor performance, which is due to the similar reason.

Stem length of H2 plays a vital role in the control of the background signal. Hairpins DNA in CHA circuits could generate an incorrect folding according to previous work [8]. In our prepared DNA biosensor, the incorrect folding resulted in circuit leakage of CHA circuits [34] and then non-specifically initiated the YNEASA circuits, which caused background signal. Specifically, hairpin H2 of incorrect folding in Fig. S-5 exposed the enzyme recognition sequences (domain 4 and 6*) that might potentially hybridize with H1 to initiate the CHA circuits as well as with MB1 to trigger the YNEASA circuits. To address this issue, stem length of H2 was optimized, as shown in Fig. S-4D. When the stem length of H2 changes from 11 to 12 nt, the background signal sharply decreases and signal-background ratio obviously increases from 3.4 to 5.4. As the stem length of H2 is longer than 12 nt, both the signal and background decrease. As is known, CHA circuits are built based on the principle of toehold-mediated strand reaction, where toehold length determines rate constants. When stem length of H2 prolong, the toehold length in H2 become shorter, causing the decreased efficiency of CHA circuits. Finally, H2-12 with stem length of 12 nt was selected for the following experiments.

3.4. Kinetic analysis of DNA biosensors

Time-dependent fluorescence analysis was performed in one-step to investigate the reaction kinetics of the three DNA biosensors based on CHA-DNEASA, the pure CHA, and CHA-YNEASA circuits. The corresponding working principle is illustrated in Fig. 3A. In CHA-DNEASA circuits, TB with enzyme recognition sequences replaced the MB1. In pure CHA circuits, the nicking enzyme was not added. To keep the same experimental conditions, the fluorescence intensity was measured for 1.5 h in response to 2 nM p53 gene activation. As shown in Fig. S-6, both CHA-DNEASA and CHA-YNEASA circuits exhibit large acceleration of fluorescence enhancement in presence of p53 gene than the pure CHA circuits, which indicates that dual signal amplification strategies improve reaction rate. Meanwhile, it is obvious that CHA-YNEASA circuits result in a weaker fluorescence signal comparing with the CHA-DNEASA circuits in absence of p53 gene, demonstrating that MB1 has a stronger ability to control nonspecific background than TB. To verify the speed-up and background control of CHA-YNEASA circuits, time-dependent signal-to-background ratio was calculated by F/F_0, as shown in Fig. 3B. An optimal signal-background ratio of 7.9 in CHA-YNEASA circuits was obtained at 23 min, where the signal-background ratio is 7 and 2 times higher than that of CHA-DNEASA and pure CHA circuits, respectively, and the reaction time is only half of that for pure CHA circuits. Hence, the CHA-YNEASA circuits significantly can shorten the reaction time, and improve signal-to-background ratio as well as facilitate the analysis process. After 23 min, signal-background ratio of CHA-YNEASA circuits decreased. The reason is that reaction rate of the CHA-YNEASA circuits in presence and absence of p53 gene gradually decreased and remained constant, respectively, as shown in Fig. S–6C. Thus, the optimal reaction time of 23 min was selected for the following experiments.

The superiorities of DNA biosensor based on CHA-YNEASA circuits are further discussed below. Obviously, the dual signal amplification strategies, such as CHA-DNEASA circuits and CHA-YNEASA circuits, have better performance than single circuits of the pure CHA circuits due to a cascade reaction and higher order signal amplification in the former. Because of almost zero background in pure CHA circuits (Fig. S–6B), the major background signal in the dual signal amplification strategies could be from NEASA circuits. In CHA-DNEASA circuits and CHA-YNEASA circuits, enzyme recognition sequences are blocked in the stem of hairpin DNA. However, the single-stranded taqman probes are so free that could invade the hairpins, causing incorrect initiation of DNEASA circuits. Thus, CHA-DNEASA circuits exhibit a low signal-

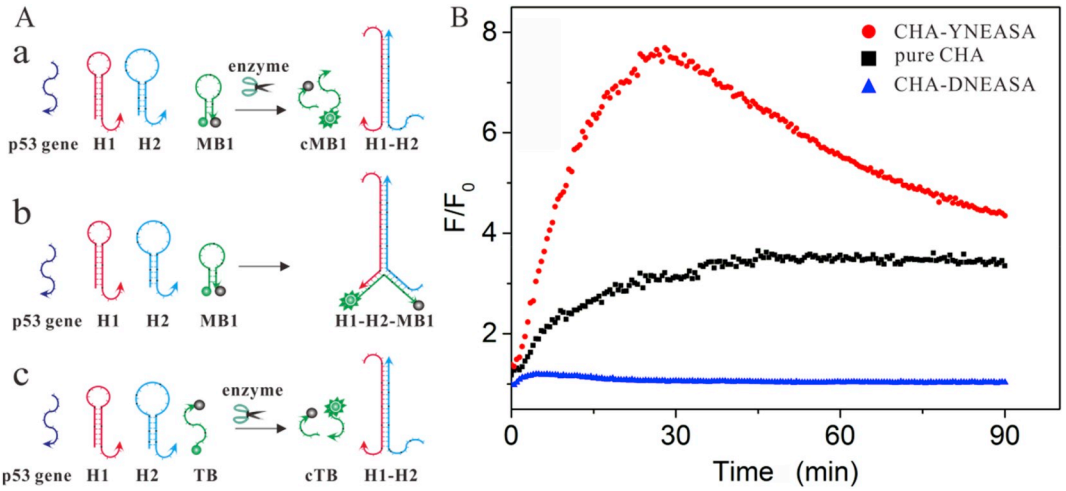

Fig. 3. Kinetic analysis of DNA biosensors. (A), Schematic diagram of DNA biosensors based on CHA-YNEASA circuits (a), pure CHA circuits (b) and CHA-DNEASA circuits (c). (B), Time-dependent signal-to-background ratio based on CHA-DNEASA circuits (red dots), pure CHA circuits (black dots) and CHA-DNEASA circuits (blue dots). F and F_0 are fluorescence intensity at 522 nm in presence and absence of 2 nM p53 gene, respectively. (For interpretation of the references to colour in this figure legend, the reader is referred to the Web version of this article.)

background ratio and aren't suitable to design biosensor. In CHA-YNEASA circuits, the degree of freedom in hairpin MB1 is limited, which avoids nonspecific hybridization between MB1 and hairpin DNA (H1 or H2-12). Moreover, YNEASA circuits is efficiently initiated only when enzyme recognition sequences are close to enzyme assisted sequence to form Y-junction DNA structure [27,29]. Thus, single hairpin DNA (H1 or H2) barely causes YNEASA circuits. MB1-concatenated dual signal amplification strategies improve reaction efficiency and accelerate reaction speed in DNA biosensor.

3.5. DNA biosensor for p53 gene detection

To compare the abilities of DNA biosensors based on pure CHA circuits or CHA-YNEASA circuits, their performance was evaluated. As shown in Fig. 4A and C, a gradual increase in fluorescence spectra was obtained corresponding to the increase of p53 gene concentration. In CHA-YNEASA circuits (Fig. 4C), the net fluorescence intensity ($F–F_0$) at 522 nm varies linearly over the p53 gene concentrations from 5 pM to 2 nM with a limit of detection (LOD) of 0.9 pM ($3\sigma/S$, where σ and S present ratio of signal to background signal and the slope of linear curve, respectively). The LOD of the CHA-YNEASA circuits was about 11-fold lower than that of the pure CHA circuits (Fig. 4B and D). Moreover, compared with the other reported works for p53 gene detection as listed in Table S2, our proposed DNA biosensor based on the CHA-YNEASA circuits exhibits higher sensitivity and shorter reaction time.

The specificity of the DNA biosensor was carried out. Five kinds of mismatched DNAs were selected as control groups and the corresponding sequences are listed in Table S1. As depicted in Fig. S-7, the DNA biosensor was unresponsive to both of single-mismatched and double-mismatched p53 genes. Therefore, our proposed DNA biosensor has a strong capability to discriminate mismatched DNA sequences.

The practical application of the DNA biosensor was carried out in human serum spiked p53 gene with various concentrations (West China Hospital of Sichuan University ethical clearance letter number: K2017039). As displayed in Table 1, the spiked recovery was obtained within the range from 95% to 102% and the relative standard deviation (RSD) in all groups was below 8.5%. The results demonstrate that our prepared DNA biosensor offers a well anti-interference ability in complex matrix.

3.6. Adaption of DNA biosensor for cytosensor design

Apart from genes at nucleic acid levels, our prepared DNA biosensor based on CHA-YNEASA circuits is also adaptative for detection of cancer cells at cell level. At early stage, rare cancer cells spread and travel through the bloodstream [35]. Thus, cancer cell measurement also provides another important way for cancer clinical diagnosis. To construct a cytosensing, hairpin apt@Is was integrated into CHA-YNEASA circuits using the modularity principle in Fig. 5, and the corresponding sequences were designed according to the process in Figure S-1. Initiation of the CHA-YNEASA circuits was precisely adjusted by control the conformation of hairpin apt@Is. Hairpin apt@Is contains a initiation strand to trigger CHA-YNEASA circuits, and a MUC1 aptamer that binds to MCF-7 cancer cells with high affinity and specificity due to high expression level of MUC1 protein on its cell membrane [36]. Thus, the CHA-YNEASA circuits occur on the surface of cell membrane. As we known, rare hairpin DNAs can transport across cell membrane. The aim of proposed biosensors is to achieve cancer diagnosis *in vitro* rather than *in vivo*. Thus, cytotoxicity of CHA-YNEASA circuits was not explored here. As a proof-to-concept, CHA-YNEASA circuits triggered by initiation strand (Is) were tested by PAGE imaging at first. Fig. S-8 shows the similar results as those in Fig. 2B, which illustrates that CHA-YNEASA circuits are effectively initiated by Is. Moreover, the fragments (cMB2) were observed in lines 7–9, which was caused by the fact that one of cMB2 folded into hairpin DNA structure and its stem were stained by 4 S Red Plus Nucleic Acid Stain. Thus, the DNA biosensor based on CHA-YNEASA circuits is adaptative for detection of other nucleic acids. Then, the feasibility of CHA-YNEASA circuits triggered by cancer cells was verified. As shown in Fig. S-9, the fluorescence intensity was higher in presence of MCF-7 cancer cells (curve b) than that in absence of MCF-7 cancer cells (curve a). The results demonstrate that the binding between cancer cells and apt@Is change its conformation and expose Is to trigger CHA circuits. When nicking enzyme was added, fluorescence intensity was remarkably increased in curve d, indicating that both the two circuits were triggered. Therefore, DNA biosensor is adaptative for designing a cytosensor.

To obtain the optimal performance, four different stem lengths of apt@Is listed in Table S1 were synthesized. As shown in Fig. S-10, the free energy of secondary structures decrease and hairpin structure become more stable as stem of apt@Is get longer. Fig. S-11 shows the performance of cytosensing by using four kinds of apt@Is. When the stem was extended, the structure of apt@Is was fixed thereby unable to

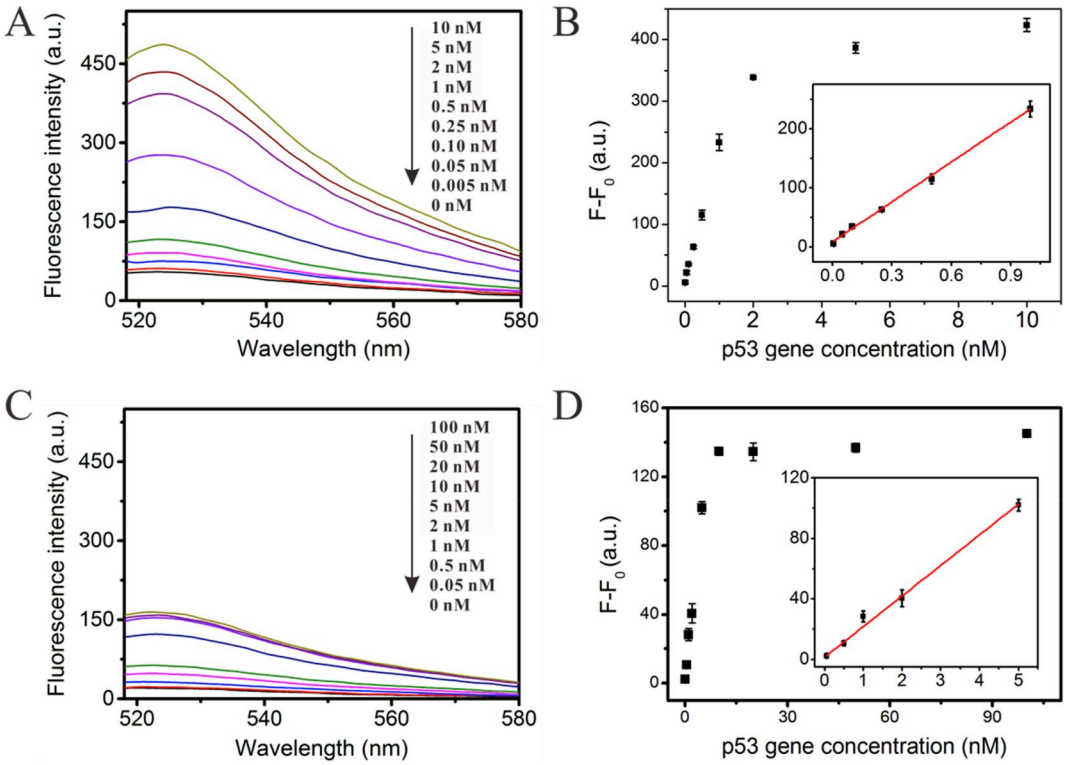

Fig. 4. Performance evaluations of DNA biosensors for p53 gene detection. Fluorescence profile corresponding to p53 gene concentrations in DNA biosensor based on CHA-YNEASA circuits (A) and pure CHA circuits (C). Relative fluorescence intensity in response to p53 gene at various concentrations and their calibration curves (inset image) in DNA biosensor based on CHA-YNEASA circuits (B) and pure CHA circuits (D). Inset: P53 gene concentrations range from 1 nM to 0.005 nM (B) and from 5 nM to 0.05 nM (D), respectively. The linear relationship in DNA biosensor based on CHA-YNEASA circuits and pure CHA circuits can be described as $F–F_0 = 219.6\ C + 9.5$ (correlation coefficient, 0.993) and $F–F_0 = 20.2\ C + 1.4$ (correlation coefficient, 0.992), respectively, where F and F_0 are fluorescence intensity at 522 nm in presence and absence of 2 nM p53 gene respectively, C is p53 gene concentration.

Table 1
Real sample assays in human serum for p53 gene detection.

Samples	p53 gene (nM)	Assay results (nM)	Recovery (%)	RSD (%)
1	0.050	0.051	102%	8.36%
2	0.250	0.244	98%	3.60%
3	1.000	0.953	95%	3.40%

bind with cancer cells, leading to weak fluorescence signal. However, when the stem shortened, background signal was increased since the decreased thermal stability of apt@Is could mistrigger the assembly of CHA-YNEASA circuits. Therefore, apt@Is-3 was chose for the following experiment.

The performance of the cytosensor was assessed by using MCF-7 cancer cells as a mode target. Fig. 6A displays the fluorescence spectra of the designed cytosensor at different concentrations of MCF-7 cancer cells. The fluorescence intensity clearly shows a gradual enhancement with an increasing concentration of MCF-7 cancer cells. The net fluorescence intensity ($F–F_0$) at 522 nm, calculated by subtracting the fluorescence intensity in binding buffer (F_0), was linearly proportional to the MCF-7 cancer cell concentration over the range of 1×10^2–1×10^4 cells/mL with low limit of detection of 100 cells/mL, as shown in Fig. 6B. Taking into account of reaction volumes of 130 μL, detection amounts of cancer cells in reaction system are calculated as 13 cells, which are comparable to that of some reported cytosensors [37–39].

Specificity is a vital parameter in performance evaluation of cytosensor. The analytical signals of the MCF-7 cancer cells were compared with the control groups, containing normal cells (HL-7702) and the MUC1 negative cancer cells (SW620, Hep G2 and U–2OS), as shown in Fig. 6C. In the absence of MUC1 on the cell membrane surface, the

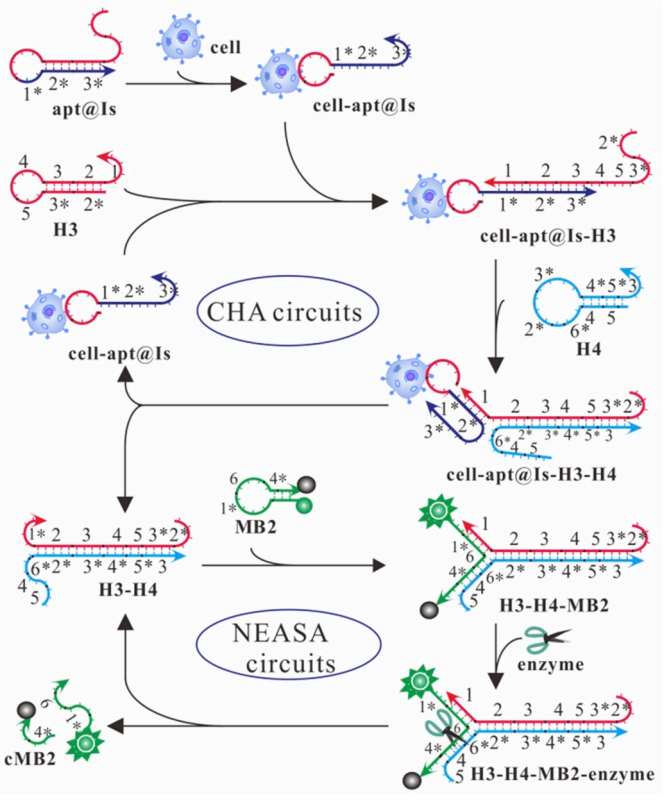

Fig. 5. Working principle of cytosensor based on CHA-YNEASA circuits.

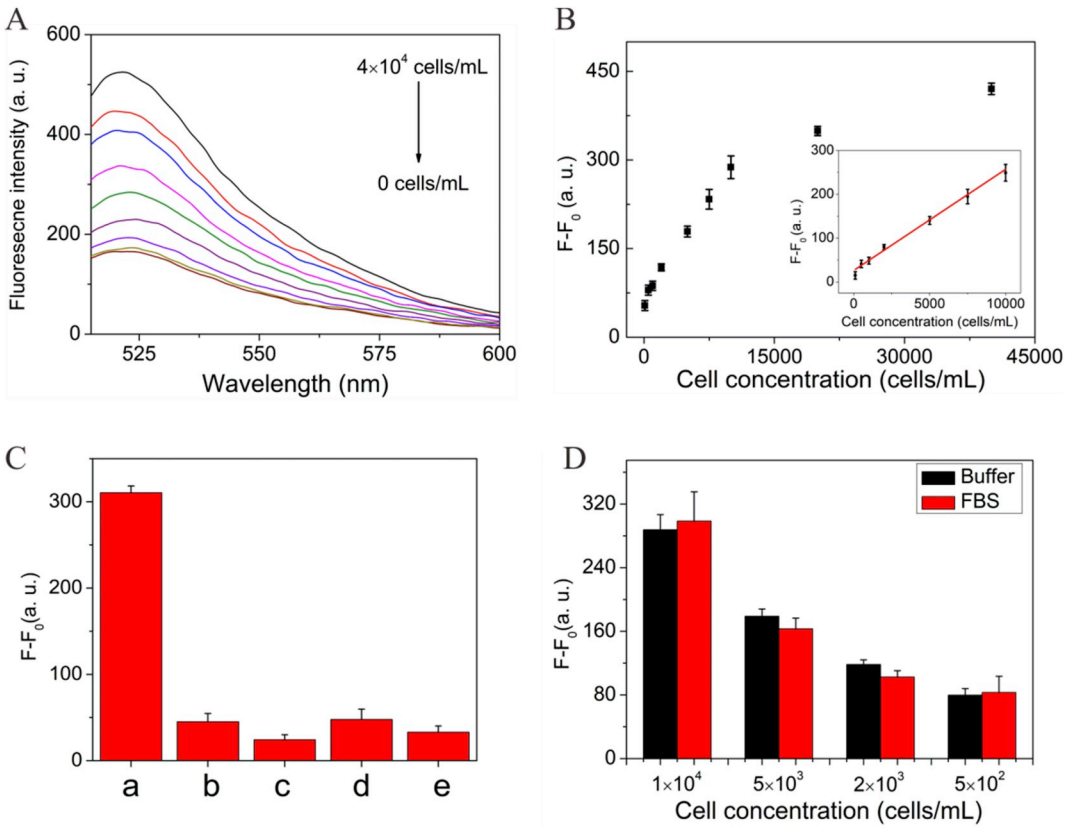

Fig. 6. Performance evaluations of cytosensor based on CHA-YNEASA circuits. (A) Fluorescence profile corresponding to different concentrations of MCF-7 cancer cells (from top to bottom: 4×10^4, 2×10^4, 1×10^4, 7.5×10^3, 5×10^3, 2×10^3, 1×10^3, 5×10^2, 1×10^2, 0 cells/mL). (B) Relative fluorescence intensity in response to MCF-7 cancer cells at various concentrations (from 4×10^4 to 1×10^2 cells/mL) and their calibration curves (inset image: from 1×10^4 to 1×10^2 cells/mL). Linear regression equation: $F–F_0 = 0.023\ C_{cell} + 26.409$, $R^2 = 0.98$. Linear range was from 1×10^2 to 1×10^4 cells/mL. (C) Specificity of MCF-7 cancer cells against different kinds of cell lines at concentration of 2×10^4 cells/mL: (a) MCF-7, (b) SW620, (c) U–2OS, (d) HL-7702, (e) Hep G2, (f) blank solution (without cell). Error bars represent standard deviation (n = 3). (D) Fluorescence assay results of MCF-7 cancer cell detection in 10% FBS (red) and in PBS buffer (black) using cytosensor based on CHA-YNEASA. (For interpretation of the references to colour in this figure legend, the reader is referred to the Web version of this article.)

binding between the MUC1 negative cell and MUC1 aptamer is not allowed. In the group of normal cells or the MUC1 negative cancer cells, the structure-switch of hairpin apt@Is was on an off state and the CHA-YNEASA circuits were prohibited. Strong signals were observed only for the MUC1 positive cancer cells (MCF-7), which indicates that the cytosensor exhibits an excellent specificity to efficiently distinguish the MCF-7 breast cancer cells from the other cells. The potential application of the cytosensor for MCF-7 cell detection in complex matrix was performed by spiked experiments. MCF-7 at various concentrations was spiked in 10% FBS and then was analyzed by the proposed protocol. As shown in Fig. 6D, the fluorescence signal in 1 × CutSmart™ buffer is similar to that in 10% FBS, confirming that the DNA biosensor-based cytosensor shows a good anti-interference ability. Hence, the proposed DNA biosensor has great potential to construct cytosensors for clinical application of cancer cell detection.

4. Conclusion

A simple, rapid, sensitive DNA biosensor based on CHA-YNEASA circuits was fabricated for the first time. The CHA-YNEASA circuits with a simply system offered a strong ability to control background signal by forming a Y-junction structure. Hence, DNA biosensor was able to simply operate in just one-step process with a high signal-to-background ratio. Moreover, the DNA biosensor was successfully applied into p53 gene detection with high sensitivity (a LOD of 0.9 pM), showing the merits of short analysis time (23 min) and excellent identification capability for base mismatch. In addition, the DNA biosensor was adaptative for constructing a cytosensor through using apt@Is as a switch. A high detection limit of 13 MCF-7 cancer cells in reaction system was achieved. Noticeably, the cytosensor exhibits excellent specificity and good anti-interference. Thus, our proposed DNA biosensor offers a powerful tool for clinical diagnosis of cancer at early stage.

Zewei Luo: Methodology, Writing-original draft, Formal analysis, Funding acquisition. Ya Xu: Data curation, Formal analysis. Zhijun Huang: Formal analysis. Junman Chen: Formal analysis. Xiaqing Wang: Formal analysis. Dan Li: Formal analysis. Yongxin Li: Writing-review & editing, Funding acquisition. Yixiang Duan: Funding acquisition, Methodology, Investigation, Project administration.

Declaration of competing interest

The authors declare no competing financial interest.

Acknowledgements

This research was gratefully supported by Miaozi Project in Science and Technology Innovation Program of Sichuan Province (2019094), the National Natural Science Foundation of China (No. 21874095), the Key Research and Development Project from Department of Science and Technology, Sichuan Province (2017SZ0013), PR China, and Sichuan University Innovation Spark Project (2018SCUH0076).

Appendix A. Supplementary data

Supplementary data to this article can be found online at https://doi.org/10.1016/j.talanta.2019.120638.

References

[1] H. Deng, Y. Xu, Y.H. Liu, Z.J. Che, H.L. Guo, S.X. Shan, Y. Sun, X.F. Liu, K.Y. Huang, X.W. Ma, Y. Wu, X.J. Liang, Gold nanoparticles with asymmetric polymerase chain reaction for colorimetric detection of DNA sequence, Anal. Chem. 84 (2012) 1253–1258.

[2] R. Banerjee, C.B. Teng, S.A. Cunningham, S.M. Ihde, J.M. Steckelberg, J.P. Moriarty, N.D. Shah, J.N. Mandrekar, R. Patel, Randomized trial of rapid multiplex polymerase chain reaction-based blood culture identification and susceptibility testing, Clin. Infect. Dis. 61 (2015) 1071–1080.

[3] M. Helou, M. Reisbeck, S.F. Tedde, L. Richter, L. Bar, J.J. Bosch, R.H. Stauber, E. Quandt, O. Hayden, Time-of-flight magnetic flow cytometry in whole blood with integrated sample preparation dagger, Lab Chip 13 (2013) 1035–1038.

[4] S.M. Hanash, S.J. Pitteri, V.M. Faca, Mining the plasma proteome for cancer biomarkers, Nature 452 (2008) 571–579.

[5] J.D. Brooks, Translational genomics: the challenge of developing cancer biomarkers, Genome Res. 22 (2012) 183–187.

[7] C. Jung, A.D. Ellington, Diagnostic applications of nucleic acid circuits, Accounts Chem. Res. 47 (2014) 1825–1835.

[8] B. Li, A.D. Ellington, X. Chen, Rational, modular adaptation of enzyme-free DNA circuits to multiple detection methods, Nucleic Acids Res. 39 (2011) e110.

[9] Y.D. Tang, B.Y. Lu, Z.T. Zhu, B.L. Li, Establishment of a universal and rational gene detection strategy through three-way junction-based remote transduction, Chem. Sci. 9 (2018) 760–769.

[10] Y.H. Guo, J. Wu, H.X. Ju, Target-driven DNA association to initiate cyclic assembly of hairpins for biosensing and logic gate operation, Chem. Sci. 6 (2015) 4318–4323.

[11] W.B. Cheng, Y. Zhang, H. Yu, W. Diao, F. Mo, B. Wen, W. Cheng, Y.R. Yan, An enzyme-free colorimetric biosensing strategy for ultrasensitive and specific detection of microRNA based on mismatched stacking circuits, Sens. Actuators B Chem. 255 (2018) 3298–3304.

[12] Y.Y. Xu, W.J. Zhou, M. Zhou, Y. Xiang, R. Yuan, Y.Q. Chai, Toehold strand displacement-driven assembly of G-quadruplex DNA for enzyme-free and non-label sensitive fluorescent detection of thrombin, Biosens. Bioelectron. 64 (2015) 306–310.

[14] Y. Zang, J.P. Lei, P.H. Ling, H.X. Ju, Catalytic hairpin assembly-programmed porphyrin-DNA complex as photoelectrochemical initiator for DNA biosensing, Anal. Chem. 87 (2015) 5430–5436.

[15] Z. Chen, S. Chengjun, L. Zewei, L. Kunping, Y. Xijian, Z. Haimin, L. Yongxin, D. Yixiang, Fiber optic biosensor for detection of genetically modified food based on catalytic hairpin assembly reaction and nanocomposites assisted signal amplification, Sens. Actuators B Chem. 254 (2018) 956–965.

[16] Z.T. Zhu, Y.D. Tang, Y.S. Jiang, S. Bhadra, Y. Du, A.D. Ellington, B.L. Li, Strand-exchange nucleic acid circuitry with enhanced thermo-and structure- buffering abilities turns gene diagnostics ultra-reliable and environmental compatible, Sci. Rep. 6 (2016) 36605.

[17] Z.W. Luo, Y.M. Wang, X.Y. Lu, J.M. Chen, F.J. Wei, Z.J. Huang, C. Zhou, Y.X. Duan, Fluorescent aptasensor for antibiotic detection using magnetic bead composites coated with gold nanoparticles and a nicking enzyme, Anal. Chim. Acta 984 (2017) 177–184.

[18] Q. Liu, C. Liu, G. Zhu, H.F. Xu, X.J. Zhang, C.J. Hu, Y. Xie, K.Y. Zhang, H.Y. Wang, Electrochemiluminescent determination of the activity of uracil-DNA glycosylase: combining nicking enzyme assisted signal amplification and catalyzed hairpin assembly, Microchim. Acta 186 (2019) 179.

[19] Y. Weizmann, M.K. Beissenhirtz, Z. Cheglakov, R. Nowarski, M. Kotler, I. Willner, A virus spotlighted by an autonomous DNA machine, Angew. Chem. Int. Ed. 45 (2006) 7384–7388.

[20] Z.J. Huang, Z.W. Luo, J.M. Chen, Y. Xu, Y.X. Duan, A facile, label-free, and universal biosensor platform based on target-induced graphene oxide constrained DNA dissociation coupling with improved strand displacement amplification, ACS Sens. 3 (2018) 2423–2431.

[21] R.J. Zeng, Z.B. Luo, L.J. Zhang, D.P. Tang, Platinum nanozyme-catalyzed gas generation for pressure-based bioassay using polyaniline nanowires-functionalized graphene oxide framework, Anal. Chem. 90 (2018) 12299–12306.

[22] Y.R. Yan, B. Shen, H. Wang, X. Sun, W. Cheng, H. Zhao, H.X. Ju, S.J. Ding, A novel and versatile nanomachine for ultrasensitive and specific detection of microRNAs based on molecular beacon initiated strand displacement amplification coupled with catalytic hairpin assembly with DNAzyme formation, Analyst 140 (2015) 5469–5474.

[23] J. Chen, H.D. Qiu, M.L. Zhang, T.N. Gu, S.J. Shao, Y. Huang, S.L. Zhao, Hairpin assembly-triggered cyclic activation of a DNA machine for label-free and ultrasensitive chemiluminescence detection of DNA, Biosens. Bioelectron. 68 (2015) 550–555.

[24] F. Tao, J. Fang, Y.C. Guo, Y.Y. Tao, X.L. Han, Y.X. Hu, J.J. Wang, L.Y. Li, Y.L. Jian, G.M. Xie, A target-triggered biosensing platform for detection of HBV DNA based on DNA walker and CHA, Anal. Biochem. 554 (2018) 16–22.

[25] T.R. Kuang, L.Q. Chang, X.F. Peng, X.L. Hu, D. Gallego-Perez, Molecular beacon nano-sensors for probing living cancer cells, Trends Biotechnol. 35 (2017) 347–359.

[26] S. Feng, Y. Shang, F. Wu, F. Ding, B. Li, J.H. Xu, L. Xu, X. Zhou, DNA nanomachines as evolved molecular beacons for in vitro and in vivo detection, Talanta 120 (2014) 141–147.

[27] S.F. Liu, C.X. Zhang, J.J. Ming, C.F. Wang, T. Liu, F. Li, Amplified detection of DNA by an analyte-induced Y-shaped junction probe assembly followed with a nicking endonuclease-mediated autocatalytic recycling process, Chem. Commun. 49 (2013) 7947–7949.

[28] Y.H. Chen, S.L. Guo, M. Zhao, P. Zhang, Z.L. Xin, J. Tao, L.J. Bai, Amperometric DNA biosensor for Mycobacterium tuberculosis detection using flower-like carbon nanotubes-polyaniline nanohybrid and enzyme-assisted signal amplification strategy, Biosens. Bioelectron. 119 (2018) 215–220.

[29] R.-M. Kong, X.-B. Zhang, L.-L. Zhang, Y. Huang, D.-Q. Lu, W.H. Tan, G.-L. Shen, R.-Q. Yu, Molecular beacon-based junction probes for efficient detection of nucleic acids via a true target-triggered enzymatic recycling amplification, Anal. Chem. 83 (2011) 14–17.

[31] H.Y. Zhu, M.J. Zhang, L. Zou, R.M. Li, L.S. Ling, Sequence specific recognition of HIV-1 dsDNA in the large amount of normal dsDNA based upon nicking enzyme signal amplification and triplex DNA, Talanta 173 (2017) 9–13.

[32] C.H. Zhang, Y. Tang, Y.Y. Sheng, H. Wang, Z. Wu, J.H. Jiang, Ultrasensitive detection of microRNAs using catalytic hairpin assembly coupled with enzymatic repairing amplification, Chem. Commun. 52 (2016) 13584–13587.

[33] L.J. Bai, Y.Q. Chai, X.Y. Pu, R. Yuan, A signal-on electrochemical aptasensor for ultrasensitive detection of endotoxin using three-way DNA junction-aided enzymatic recycling and graphene nanohybrid for amplification, Nanoscale 6 (2014) 2902–2908.

[34] X. Chen, N. Briggs, J.R. McLain, A.D. Ellington, Stacking nonenzymatic circuits for high signal gain, P. Natl. Acad. Sci. USA 110 (2013) 5386–5391.

[35] H. Naderi-Meshkin, N. Ahmadiankia, Cancer metastasis versus stem cell homing: role of platelets, J. Cell. Physiol. 233 (2018) 9167–9178.

[36] L. Cai, Z.Z. Chen, M.Y. Chen, H.W. Tang, D.W. Pang, MUC-1 aptamer-conjugated dye-doped silica nanoparticles for MCF-7 cells detection, Biomaterials 34 (2013) 371–381.

[37] L. Li, X.X. Zheng, Y.Z. Huang, L.N. Zhang, K. Cui, Y. Zhang, J.H. Yu, Addressable TiO_2 nanotubes functionalized paper-based cyto-sensor with photocontrollable switch for highly-efficient evaluating surface protein expressions of cancer cells, Anal. Chem. 90 (2018) 13882–13890.

[38] M. Dervisevic, M. Senel, T. Sagir, S. Isik, Highly sensitive detection of cancer cells with an electrochemical cytosensor based on boronic acid functional polythiophene, Biosens. Bioelectron. 90 (2017) 6–12.

[39] L. Zhang, Y.Z. Wang, Q.Q. Tian, Y. Liu, J.H. Li, Multienzyme decorated polysaccharide amplified electrogenerated chemiluminescence biosensor for cytosensing and cell surface carbohydrate profiling, Biosens. Bioelectron. 89 (2017) 1013–1019.

[40] L. Jumei, et al., Bifunctional aptamer-mediated catalytic hairpin assembly for the-sensitive and homogenous detection of rare cancer cells, Anal. Chim. Acta (2018) 58–64, https://doi.org/10.1016/j.aca.2018.04.068.

[41] L. Jumei, et al., Applications of Catalytic Hairpin Assembly Reactionin Biosensing, Small (2019), https://doi.org/10.1002/smll.201902989.